

Non-Markovian dynamics revealed at a bound state in the continuum

Savannah Garmon* and Kenichi Noba

Department of Physical Science, Osaka Prefecture University, Gakuen-cho 1-1, Sakai 599-8531, Japan

Gonzalo Ordonez

Department of Physics and Astronomy, Butler University, Gallahue Hall, 4600 Sunset Avenue, Indianapolis, Indiana 46208, USA

Dvira Segal

Chemical Physics Theory Group, Department of Chemistry, University of Toronto, 80 Saint George Street, Toronto, Ontario, M5S 3H6, Canada

(Received 17 August 2018; published 11 January 2019)

We propose a methodical approach to controlling and enhancing deviations from exponential decay in quantum and optical systems by exploiting recent progress surrounding another subtle effect: the bound states in the continuum, which have been observed in optical waveguide array experiments within this past decade. Specifically, we show that by populating an initial state orthogonal to that of the bound state in the continuum, it is possible to engineer system parameters for which the usual exponential decay process is suppressed in favor of inverse power law dynamics and coherent effects that typically would be extremely difficult to detect in experiment. We demonstrate our method using a model based on an optical waveguide array experiment and further show that the method is robust even in the face of significant detuning from the precise location of the bound state in the continuum.

DOI: [10.1103/PhysRevA.99.010102](https://doi.org/10.1103/PhysRevA.99.010102)

A bound state in the continuum (BIC) represents a localized eigenmode with energy eigenvalue that, counterintuitively, resides directly within the scattering continuum of a given physical system. Although the existence of such modes was first predicted in 1929 [1], the phenomenon is so delicate that they were not observed until much more recently [2]; for example, in optical waveguide array experiments [3–6]. Lasing action has also recently been reported for a cavity supporting BICs [7]. In this paper, we propose to apply these recent technical advances in optical control of the BIC to the study of another often elusive phenomenon: long-time nonexponential decay.

In many familiar circumstances, such as atomic relaxation, we tend to think of quantum decay as essentially an exponential process. More precisely, exponential decay tends to manifest when an unstable eigenmode (such as an excited atomic level) is resonant with an energy continuum (environmental reservoir, such as the electromagnetic vacuum) to which it is coupled. However, it can be shown that, in fact, all quantum systems follow nonexponential dynamics on very short and extremely long timescales. These deviations occur as a direct result of the existence of at least one threshold on the energy continuum in such systems [8–15]. While these effects are ubiquitous in quantum systems, they are unfortunately quite difficult to detect under ordinary circumstances and hence have been measured only in a small handful of experiments [16–21]. The short-time deviation, which can give rise to both decelerated [22] and accelerated [23] decay under frequent

system observations [17,20–22] or modulation of the environmental coupling [18], requires ultraprecision to detect that is often difficult to achieve in the laboratory. Reference [24] uses the properties of a BIC to study these short-time effects.

The long-time deviation, meanwhile, has proven even more challenging [19]. The difficulty originates in that the effect usually does not appear until many lifetimes of the exponential decay have passed, by which time the survival probability is so depleted that it is rendered undetectable. A handful of theory papers have suggested special circumstances to enhance the long-time effect; these mostly require an initially prepared state near the threshold, usually combined with other conditions [13,25–32]. See also the recent experiment [33].

In this paper, we take advantage of the simple geometric shape of the BIC to present a qualitatively different and more easily generalized scheme by which the long-time deviation can be enhanced. While it is clear from the outset that the usual exponential decay associated with the resonance is suppressed when the BIC condition is satisfied, if one were to directly populate the BIC itself, then one would observe a simple stable evolution, as the BIC is of course an eigenstate of the Hamiltonian. However, we show that by populating a state that is orthogonal to the BIC we can take advantage of the suppression of the exponential effect while avoiding the stability associated with the BIC itself. The nonexponential dynamics can then drive the evolution on all timescales. What's more, we demonstrate in our example below that the exponential effect can be dramatically suppressed even with significant detuning from the BIC, although the choice of BIC-orthogonal initial state is still essential.

*sgarmon@p.s.osakafu-u.ac.jp

We illustrate our method relying on a simple tight-binding model that can be viewed analogously to one of the previously mentioned optical waveguide array experiments. Our Hamiltonian is written

$$H = \epsilon_d |d\rangle\langle d| - J \sum_{n=1}^{\infty} (|n\rangle\langle n+1| + |n+1\rangle\langle n|) - g(|d\rangle\langle 2| + |2\rangle\langle d|), \quad (1)$$

in which the second term represents the semi-infinite array with nearest-neighbor hopping parameter $-J$ and the chain is side-coupled at site $|2\rangle$ to an “impurity” element $|d\rangle$. After we set the energy units according to $J = 1$, the adjustable parameters in the system are the chain-impurity coupling $-g$ and the impurity energy level ϵ_d . This model captures the essential features of the waveguide array experiment in Ref. [6] (see Refs. [34,35]) when we view time evolution in the present context analogously to longitudinal propagation within the waveguides. This model can be partially diagonalized by introducing a half-range Fourier series on the chain according to $|n\rangle = \sqrt{\frac{2}{\pi}} \int_0^{\pi} dk \sin nk |k\rangle$, after which we have

$$H = \epsilon_d |d\rangle\langle d| + \int_0^{\pi} dk E_k |k\rangle\langle k| + g \int_0^{\pi} dk V_k (|d\rangle\langle k| + |k\rangle\langle d|), \quad (2)$$

where $V_k = -\sqrt{\frac{2}{\pi}} \sin 2k$ and the continuum is given by $E_k = -2J \cos k$ over $k \in [0, \pi]$. Note from here we will measure the energy in units of $J = 1$.

The discrete spectrum for this model can be obtained, for example, from the resolvent operator

$$\langle d| \frac{1}{z - H} |d\rangle = \frac{1}{z - \epsilon_d - \Sigma(z)}, \quad (3)$$

in which the self-energy function $\Sigma(z) = g^2 \int_0^{\pi} dk \frac{|V_k|^2}{z - E_k}$ is evaluated as

$$\Sigma(z) = \frac{zg^2}{2} [z^2 - 2 - z\sqrt{z^2 - 4}] \quad (4)$$

in the first Riemann sheet (see Ref. [36] for discussion of the analytic properties of $\Sigma(z)$). Notice that a pole occurs in Eq. (3) at $z = 0$ after choosing $\epsilon_d = 0$; this is the BIC solution for this model, which resides directly at the center of the continuum $z \in [-2, 2]$ (defined by the range of E_k) and which takes the form

$$|\psi_{\text{BIC}}\rangle = \frac{1}{\sqrt{1+g^2}} (|d\rangle - g|1\rangle). \quad (5)$$

We here emphasize that the BIC state can be understood as a resonance with vanishing decay width [2,35,37–51]. In this picture, the ordinary resonance represents a generalized eigenstate with complex energy eigenvalue, for which the imaginary part of the eigenvalue gives the exponential decay half-width. When the BIC condition $\epsilon_d = 0$ is fulfilled, the imaginary part of this eigenvalue vanishes, yielding a bound state residing directly in the scattering continuum. When $\epsilon_d \neq 0$, the complex eigenvalue is restored and the exponential decay would generally be expected to reappear.

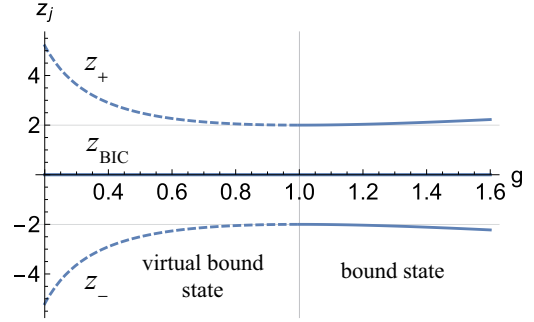


FIG. 1. Discrete spectrum of our model as a function of g in the case $\epsilon_d = 0$. The BIC appears at $z_{\text{BIC}} = 0$. The other two solutions are virtual bound states (dashed curves) for $g < 1$; they become bound states for $g > 1$. (Energy is measured in units of $J = 1$ throughout the paper.)

It is easy to show that there exist two further solutions for the $\epsilon_d = 0$ case with eigenvalues given by $z_{\pm} = \pm z_g$, in which

$$z_g = g + \frac{1}{g}. \quad (6)$$

For $g > 1$, these two solutions constitute localized bound states residing on the first Riemann sheet of the complex energy plane, while for $g < 1$ they transition to so-called virtual bound states (or antibound states), which are delocalized pseudostates with real eigenvalue resting in the second sheet [13,31,52–55], see Fig. 1. While the virtual bound states do not appear in the diagonalized Hamiltonian, they nevertheless have a similar influence on the long-time power law decay as do the bound states [13]. Specifically, we will show that the timescale characterizing the nonexponential decay is proportional to Δ_g^{-1} , where

$$\Delta_g \equiv z_g - 2 \quad (7)$$

is defined as the gap between either of the (virtual) bound state energies and the nearest band edge. Note we will particularly focus on the $g \leq 1$ portion of the parameter space as the absence of bound states here means that nothing inhibits the nonexponential decay. (For comparison, we will also briefly discuss the $g > 1$ evolution.)

As previously discussed, if we were to consider the evolution of the BIC state itself, the initial state would simply remain occupied for all time as $|\psi_{\text{BIC}}\rangle$ is an eigenstate of H with energy eigenvalue $z = 0$. However, by instead choosing the (simplest) BIC-orthogonal state

$$|\psi_{\perp}\rangle = \frac{1}{\sqrt{1+g^2}} (g|d\rangle + |1\rangle) \quad (8)$$

as our initial state, we obtain complete nonexponential decay for any value $g \leq 1$, as shown below.¹ To analyze the evolution of $|\psi_{\perp}\rangle$, we evaluate the survival probability

¹One might pause at the inclusion of the site $|1\rangle$ that is technically part of the reservoir in this initial state. However, $|1\rangle$ could equivalently be viewed as a second impurity element [36].

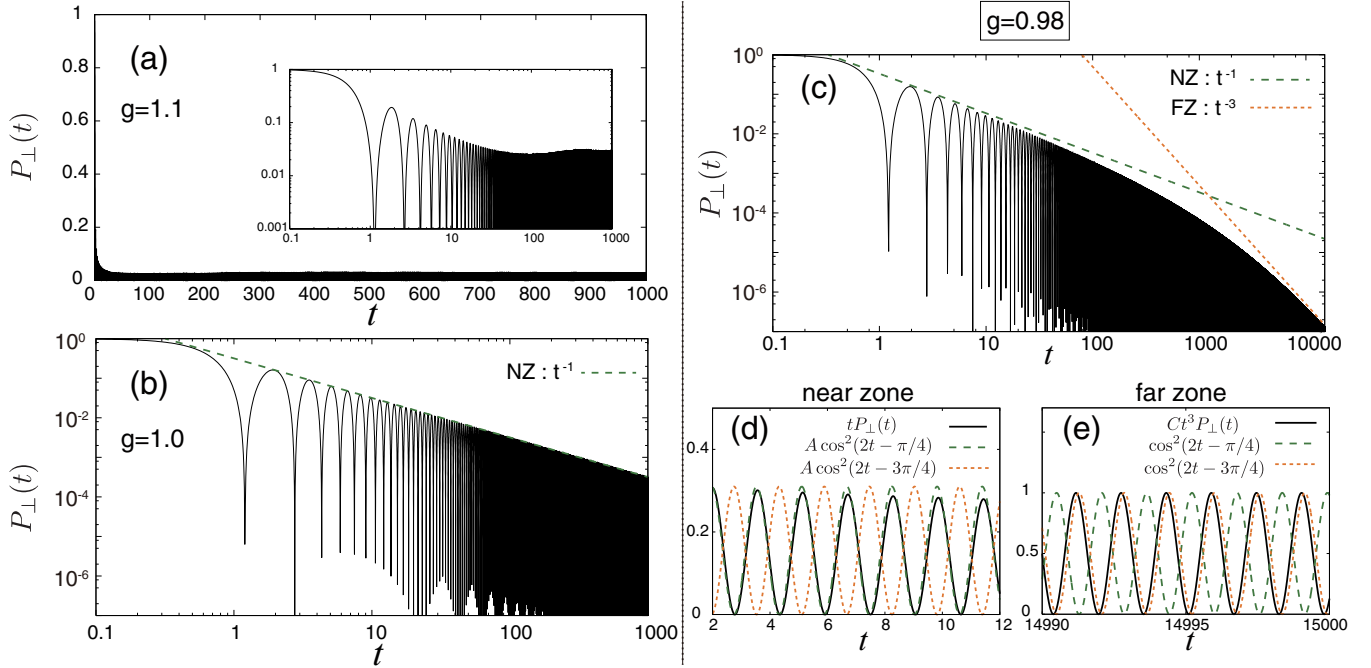


FIG. 2. Numerical simulations for the survival probability of $|\psi_{\perp}\rangle$ at time t for $\epsilon_d = 0$ and (a) $g = 1.1$ (linear plot, inset: log-log plot), (b) $g = 1.0$ (log-log plot), and (c), (d), (e) $g = 0.98$ [(c) log-log plot, (d) early near zone close-up, and (e) far zone close-up]. The green dashed (orange dotted) lines indicate the $1/t$ ($1/t^3$) dynamics. The numerical method is described in Ref. [36]. (Time t is measured in units $1/J$ in which $J = 1$.)

$P_{\perp}(t) = |A_{\perp}(t)|^2$, in which the survival amplitude is given by

$$\begin{aligned} A_{\perp}(t) &= \langle \psi_{\perp} | e^{-iHt} | \psi_{\perp} \rangle \\ &= \frac{1}{2\pi i} \int_{\mathcal{C}_E} e^{-izt} \langle \psi_{\perp} | \frac{1}{z - H} | \psi_{\perp} \rangle dz. \end{aligned} \quad (9)$$

Here \mathcal{C}_E is a counterclockwise integration contour surrounding the real axis in the first Riemann sheet of the complex energy plane, which includes the branch cut along $z \in [-2, 2]$ as well as any bound states. We can apply various methods to evaluate this integral; for example, by directly computing the relevant matrix elements of the resolvent operator and integrating over these or by applying an expansion in terms of the eigenstates of the generalized discrete spectrum of the model as in Ref. [55]. By either method, we obtain the following results.

For the case $g > 1$, there are two bound states included in the contour for Eq. (9). The survival amplitude in this case evaluates as

$$A_{\perp}(t) = \frac{g^2 - 1}{g^2} \cos z_g t + A_{\text{br}}(t), \quad (10)$$

in which the first term represents the combined contributions from the two bound states while

$$A_{\text{br}}(t) = \frac{1 + g^2}{4\pi i g^2} \int_{\mathcal{C}_{\text{br}}} dz e^{-izt} \frac{\sqrt{z^2 - 4}}{z^2 - z_g^2}. \quad (11)$$

is an integration along the contour \mathcal{C}_{br} surrounding the branch cut in a counterclockwise manner in the complex energy plane. The decay in this case is nonexponential but incomplete due to the presence of the bound states [25–27]. This can be seen for the case $g = 1.1$ in Fig. 2(a).

Meanwhile, for the case $g \leq 1$, the bound states have become virtual bound states and the evolution is now determined entirely by the non-Markovian branch cut contribution $A_{\perp}(t) = A_{\text{br}}(t)$. We find that this expression yields two distinct time regions, in which the integral is most easily estimated by somewhat different methods. First there is a short/intermediate time region, in which we first apply a fraction decomposition to the denominator of Eq. (11); this yields two simpler integrals, one associated with the upper virtual bound state and the other associated with the lower. As outlined in Ref. [36], these two integrals can be evaluated in terms of Bessel functions by methods similar to those used in Ref. [32], which yields

$$A_{\text{br}}(t) \approx \frac{1}{g} J_0(2t) - \frac{1-g}{g} \cos 2t; \quad (12)$$

this expression holds for all $t \ll T_{\Delta}$ where T_{Δ} is written as $T_{\Delta} = 1/\Delta_g = g/(1-g)^2$ in terms of the energy gap between the virtual bound states and their respective nearby band edges. On the earliest timescale $t \ll T_Z$ with $T_Z = 1$, this expression yields the usual short-time parabolic dynamics $P_Z(t) \approx 1 - Ct^2$, in which $C = (g + g^2 + g^3 - 1)/g^2$.

Then, in the intermediate time region $T_Z \ll t \ll T_{\Delta}$, we can approximate the Bessel function in the first term of Eq. (12) to write

$$A_{\text{NZ}}(t) \approx \frac{\cos(2t - \pi/4)}{g\sqrt{\pi t}} - \frac{1-g}{g} \cos 2t. \quad (13)$$

We refer to this time region including characteristic $1/t$ decay as the *nonexponential near zone* (NZ) [13], which we can roughly think of as having replaced the usual exponential decay regime. For values $g \lesssim 1$ fairly close to the $g = 1$

localization transition, the first term in Eq. (13) tends to dominate the evolution early in the near zone, while the second term provides only a small correction. Estimating the evolution in this case yields

$$P_{\text{NZ,early}}(t) \approx \frac{\cos^2(2t - \pi/4)}{\pi g^2 t}, \quad (14)$$

which can be seen for the case $g = 0.98$ in Figs. 2(c) and 2(d). As we move later into the near zone, the first term decays sufficiently so that the second term becomes nonnegligible; we can estimate this as when the second term is about 10% of the first, which gives $t = T_{\text{VR}} \sim 1/[100\pi(1-g)^2] = 1/[100\pi g] \times T_{\Delta}$. This implies we should be fairly close to the transition point $g = 1$ to observe the pure $1/t$ dynamics. For example, in the case $g = 0.98$ shown in Fig. 2(d), we can already see a small influence from the second term of Eq. (13) around $t \gtrsim T_{\text{VR}} \approx 8.0$ as the last three visible oscillation cycles show a slight deviation from the Eq. (14) prediction, which the second term of Eq. (13) [not shown] captures very well. We will return to the physical interpretation of this second term momentarily.

Next appears the asymptotic time region $T_{\Delta} \ll t$ during which the dynamics are instead described by a $1/t^3$ power law decay. To show this, we return to the (exact) integral expression for the survival amplitude appearing in Eq. (11) and instead proceed by deforming the contour C_{br} surrounding the branch cut by dragging it out to infinity in the lower half of the complex energy plane, as described in Ref. [36].

Following this procedure, we obtain

$$P_{\text{FZ}}(t) \approx \frac{(1+g^2)^2 \cos^2(2t - 3\pi/4)}{\pi g^4 \Delta_g^2 (2+z_g)^2 t^3}, \quad (15)$$

with the characteristic $1/t^3$ decay that is typical of odd dimensional systems on long timescales [13,56–60]. We refer to this as the *nonexponential far zone* (FZ). The far zone dynamics can be seen for the $g = 0.98$ case in Figs. 2(c) and 2(e).

We emphasize three further points about these results as follows. First, we draw attention more carefully to the occurrence of oscillations in both time zones, which are due to interference between the contributions from the two band edges. These contributions are equally weighted because the BIC occurs at the center of the continuum band in the present case. Notice further that a $\pi/2$ phase shift occurs between the early near-zone result Eq. (14) and the far-zone Eq. (15). These oscillations and the resulting phase shift are highlighted in Figs. 2(d) and 2(e). While similar oscillations have been previously predicted in the far zone [30,32,60], we believe the near-zone oscillations as well as the resulting phase shift are new—indeed, outside of our choice for the initial state, these would almost certainly be obscured by the exponential decay. Second, we return our attention to the second term of Eq. (13), which becomes relatively more pronounced later in the near zone; however, counterintuitively perhaps, it vanishes in the far zone.² Notice this term takes the form of a Rabi-like oscillation between the band edges at $z = \pm 2$. We refer to this effect as a *virtual Rabi oscillation*, which is intended to

reflect its transient nature. A further interesting point is that the virtual Rabi oscillation plays a role in facilitating the phase shift from the early near zone into the far zone [36].

Third, notice that when we are directly at the localization transition at $g = 1$, the second term in Eq. (13) vanishes. Further, since the key timescale T_{Δ} is inversely proportional to Δ_g , as we approach $g = 1$ from below the energy gap Δ_g closes and T_{Δ} diverges. Hence, in this case, Eq. (14) describes the dynamics accurately for all $T_Z \ll t$, which is shown in Fig. 2(b) (see also Ref. [13] for discussion relevant to this point as well as the influence of a virtual bound state on the power law decay). We can quantify the divergence of the timescale T_{Δ} in terms of the distance δ from the transition point $g = 1$ after reparameterizing according to $g \equiv 1 - \delta$; then the timescale diverges like $T_{\Delta} \sim 1/\delta^2$ as $\delta \rightarrow 0$.

While the preceding analysis gives a clear picture of the types of evolution we can expect for the state $|\psi_{\perp}\rangle$, it is still a bit idealized in comparison to experiment in two ways that we will account for below. First, in a real experiment it would be difficult to tune exactly to the BIC at $\epsilon_d = 0$; since the BIC is just the special case of a resonance with zero decay width, as we introduce detuning $\epsilon_d \neq 0$ the resonance must reappear, which we could expect might perturb the nonexponential evolution of $P_{\perp}(t)$. The complex eigenvalue of the resonance state can be expanded in the vicinity of the BIC up to second order in ϵ_d as $z_{\text{res}} \approx \epsilon_d/(1+g^2) - i\Gamma/2$ with $\Gamma = 2g^2\epsilon_d^2/(1+g^2)^3$, which of course reduces to $z_{\text{BIC}} = 0$ in the limit $\epsilon_d = 0$. However, when we examine $P_{\perp}(t)$ (red curve in Fig. 3 for $g = 0.9$, as an example), we find that the resonance has virtually no influence on the survival probability, even for moderately large detuning values $\epsilon_d \neq 0$. We can obtain an understanding for this by calculating the resonance pole contribution to $P_{\perp}(t)$. Performing first a simple calculation for the pole contribution to the amplitude $\langle \psi_{\perp} | e^{-iHt} | \psi_{\perp} \rangle$ reveals that, due to the geometric shape of the BIC-orthogonal state, both the lowest order and next-lowest order contributions in ϵ_d cancel out, which yields

$$P_{\perp,\text{res}}(t) \approx \frac{g^4 \epsilon_d^4}{(1+g^2)^8} e^{-\Gamma t}. \quad (16)$$

The prefactor in this expression, which is fourth order in ϵ_d , assures that the exponential effect will be quite small for almost any $\epsilon_d \simeq 0$ regardless of the value of g . For example, even for modest detuning $\epsilon_d = 0.2$ and $g = 0.9$ in Fig. 3(b) [red curve], we have $g^4 \epsilon_d^4 / (1+g^2)^8 \sim 10^{-5}$.

Second, while preparation of the initial state $|\psi_{\perp}\rangle$ seems feasible, measuring the precise output state $\langle \psi_{\perp} |$ might prove more challenging. Instead, it may be more realistic to consider the quantity

$$P_{1d}(t) \equiv |\langle 1 | e^{-iHt} | \psi_{\perp} \rangle|^2 + |\langle d | e^{-iHt} | \psi_{\perp} \rangle|^2, \quad (17)$$

which is equivalent to the *nonescape probability* that has appeared in the literature previously [12,57–59,61]. It can easily be shown that $P_{1d}(t) = P_{\perp}(t)$ for the case $\epsilon_d = 0$, and hence all of our preceding detailed analytical results still apply directly at the BIC. As shown in Fig. 3, the difference between $P_{1d}(t)$ [blue curve] and $P_{\perp}(t)$ [red curve] appears first well into the long-time region for small $\epsilon_d \neq 0$ and moves gradually to earlier times as we increase the detuning. The

²The reason for this is discussed in pp. 21–22 of Ref. [55].

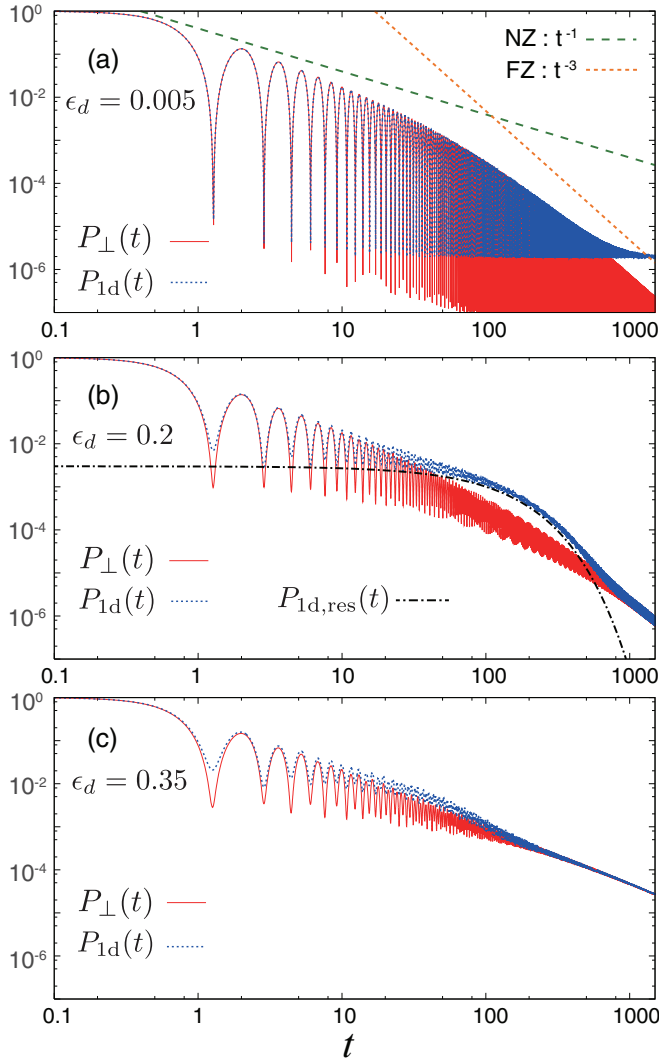


FIG. 3. Numerical simulations for the survival probability and the nonescape probability for detuning from the BIC for $g = 0.9$ and (a) $\epsilon_d = 0.005$, (b) $\epsilon_d = 0.2$, and (c) $\epsilon_d = 0.35$. (Time t is measured in units $1/J$ in which $J = 1$.)

origin of the difference between the two quantities is easy to understand as it seems to be entirely attributable to the fact that only the lowest-order contribution in ϵ_d cancels out when we calculate the resonance pole contribution to the amplitude

for the nonescape probability $P_{1d}(t)$. In particular, we find

$$P_{1d,\text{res}}(t) \approx \frac{g^2 \epsilon_d^2}{(1 + g^2)^4} e^{-\Gamma t}, \quad (18)$$

which is still small, but has some noticeable influence on the spectrum in some cases. For example, in Fig. 3(b) for $\epsilon_d = 0.2$, we see the resonance pole with magnitude $g^2 \epsilon_d^2 / (1 + g^2)^4 \sim 0.003$ introduces exponential dynamics into $P_{1d}(t)$ around $t \gtrsim 10$, although this only lasts for a few lifetimes $\tau = 2/\Gamma \sim 360$, which leaves the nonescape probability relatively intact when this quantity rejoins with $P_{\perp}(t)$ as the $1/t^3$ far-zone dynamics kick in. We note that $P_{1d}(t)$ also exhibits the interesting feature of *pre*-exponential decay that extends beyond the usual parabolic dynamics in the region $1 \lesssim t \lesssim 10$. As we further increase ϵ_d as in Fig. 3(c), we find the exponential decay region lasts even fewer lifetimes as the difference between $P_{1d}(t)$ and $P_{\perp}(t)$ again becomes diminished.

In this paper, we have shown that by populating a state that lies orthogonal to a BIC one can observe nonexponential dynamics that are usually overwhelmingly suppressed when the resonance condition is satisfied. Note that for the present model, we could consider the evolution of more general BIC orthogonal states such as $g|d\rangle + |1\rangle + \sum_{n=2}^{\infty} w_n |n\rangle$ that include elements of the chain beyond the BIC sector. We briefly comment on a representative example of this more general configuration in Ref. [36], where we show that including a single site from the chain can suppress oscillations in the survival probability.

We briefly note we have focused here on bound states in the continuum that appear purely due to interference effects as originally proposed by von Neumann and Wigner in 1929 [1]. We have not directly addressed “accidental” BICs [62] that exhibit interesting topological properties [2,7,63,64], although the study of BIC-orthogonal states in this context might prove fruitful as well.

The authors wish to thank M. V. Berry, J. G. Muga, and K. Nishidai for helpful discussions and encouragement related to this project. This work was supported in part by Japan Society for the Promotion of Science KAKENHI Grants No. JP18K03466 and No. JP16K05481. S.G. also acknowledges support from the Research Foundation for Opto-Science and Technology. D.S. acknowledges support from the Canada Research Chair Program.

[1] J. von Neumann and E. Wigner, *Phys. Z.* **30**, 465 (1929).
 [2] C. W. Hsu, B. Zhen, A. D. Stone, J. D. Joannopoulos, and M. Soljačić, *Nat. Rev. Mater.* **1**, 16048 (2016).
 [3] F. Dreisow, A. Szameit, M. Heinrich, R. Keil, S. Nolte, A. Tünnermann, and S. Longhi, *Opt. Lett.* **34**, 2405 (2009).
 [4] Y. Plotnik, O. Peleg, F. Dreisow, M. Heinrich, S. Nolte, A. Szameit, and M. Segev, *Phys. Rev. Lett.* **107**, 183901 (2011).
 [5] G. Corrielli, G. Della Valle, A. Crespi, R. Osellame, and S. Longhi, *Phys. Rev. Lett.* **111**, 220403 (2013).
 [6] S. Weimann, Y. Xu, R. Keil, A. E. Miroschnichenko, A. Tünnermann, S. Nolte, A. A. Sukhorukov, A. Szameit, and Y. S. Kivshar, *Phys. Rev. Lett.* **111**, 240403 (2013).

[7] A. Kodigala, T. Lepetit, Q. Gu, B. Bahari, Y. Fainman, and B. Kanté, *Nature* **541**, 196 (2017).
 [8] L. A. Khal'fin, *Sov. Phys. JETP* **6**, 1053 (1958).
 [9] R. G. Winter, *Phys. Rev.* **123**, 1503 (1961).
 [10] L. Fonda, G. C. Ghirardi, and A. Rimini, *Rep. Prog. Phys.* **41**, 587 (1978).
 [11] J. G. Muga, F. Delgado, A. del Campo, and G. García-Calderón, *Phys. Rev. A* **73**, 052112 (2006).
 [12] E. Torrontegui, J. G. Muga, J. Martorell, and D. W. L. Spring, *Adv. Quant. Chem.* **60**, 485 (2010).
 [13] S. Garmon, T. Petrosky, L. Simine, and D. Segal, *Fortschr. Phys.* **61**, 261 (2013).

- [14] G. Ordonez and N. Hatano, *J. Phys. A: Math. Theor.* **50**, 405304 (2017).
- [15] A. Chakraborty and R. Sensarma, *Phys. Rev. B* **97**, 104306 (2018).
- [16] S. R. Wilkinson, C. F. Bharucha, M. C. Fischer, K. W. Madison, P. R. Morrow, Q. Niu, B. Sundaram, and M. G. Raizen, *Nature (London)* **387**, 575 (1997).
- [17] M. C. Fischer, B. Gutiérrez-Medina, and M. G. Raizen, *Phys. Rev. Lett.* **87**, 040402 (2001).
- [18] A. G. Kofman and G. Kurizki, *Phys. Rev. Lett.* **87**, 270405 (2001); S. Longhi, *Opt. Lett.* **32**, 557 (2007); F. Dreisow, A. Szameit, M. Heinrich, T. Pertsch, S. Nolte, A. Tünnermann, and S. Longhi, *Phys. Rev. Lett.* **101**, 143602 (2008).
- [19] C. Rothe, S. I. Hintschich, and A. P. Monkman, *Phys. Rev. Lett.* **96**, 163601 (2006).
- [20] G. A. Álvarez, D. D. Bhaktavatsala Rao, L. Frydman, and G. Kurizki, *Phys. Rev. Lett.* **105**, 160401 (2010).
- [21] K. Kakuyanagi, T. Baba, Y. Matsuzaki, H. Nakano, S. Saito, and K. Semba, *New J. Phys.* **17**, 063035 (2015).
- [22] B. Misra and E. C. G. Sudarshan, *J. Math. Phys.* **18**, 756 (1977).
- [23] A. G. Kofman and G. Kurizki, *Phys. Rev. A* **54**, R3750 (1996); M. Lewenstein and K. Rzażewski, *ibid.* **61**, 022105 (2000); A. G. Kofman and G. Kurizki, *Nature* **405**, 546 (2000).
- [24] L. Xu, Y. Cao, X.-Q. Li, Y. J. Yan, and S. Gurvitz, *Phys. Rev. A* **90**, 022108 (2014).
- [25] A. G. Kofman, G. Kurizki, and B. Sherman, *J. Mod. Opt.* **41**, 353 (1994).
- [26] S. John and T. Quang, *Phys. Rev. A* **50**, 1764 (1994).
- [27] P. Lambropoulos, G. M. Nikolopoulos, T. R. Nielson, and S. Bay, *Rep. Prog. Phys.* **63**, 455 (2000).
- [28] T. Jittoh, S. Matsumoto, J. Sato, Y. Sato, and K. Takeda, *Phys. Rev. A* **71**, 012109 (2005).
- [29] G. García-Calderón and J. Villavicencio, *Phys. Rev. A* **73**, 062115 (2006).
- [30] S. Longhi, *Phys. Rev. Lett.* **97**, 110402 (2006).
- [31] A. D. Dente, R. A. Bustos-Marùn, and H. M. Pastawski, *Phys. Rev. A* **78**, 062116 (2008).
- [32] S. Garmon and G. Ordonez, *J. Math. Phys.* **58**, 062101 (2017).
- [33] L. Krinner, M. Stewart, A. Pazmiño, J. Kwon, and D. Schneble, *Nature* **559**, 589 (2018).
- [34] S. Longhi, *Eur. Phys. J. B* **57**, 45 (2007).
- [35] T. Fukuta, S. Garmon, K. Kanki, K.-I. Noba, and S. Tanaka, *Phys. Rev. A* **96**, 052511 (2017).
- [36] See Supplemental Material at <http://link.aps.org/supplemental/10.1103/PhysRevA.99.010102> for discussion of the analytic properties of the self-energy $\Sigma(z)$, some further details on the near zone/far zone dynamics and derivations, analysis of a more general BIC-orthogonal state, and a brief comment on the model geometry in relation to experiment.
- [37] F. H. Stillinger and D. R. Herrick, *Phys. Rev. A* **11**, 446 (1975).
- [38] H. Friedrich and D. Wintgen, *Phys. Rev. A* **31**, 3964 (1985).
- [39] M. Robnik, *J. Phys. A: Math. Gen.* **19**, 3845 (1986).
- [40] G. Ordonez, K. Na, and S. Kim, *Phys. Rev. A* **73**, 022113 (2006).
- [41] A. F. Sadreev, E. N. Bulgakov, and I. Rotter, *Phys. Rev. B* **73**, 235342 (2006).
- [42] H. Nakamura, N. Hatano, S. Garmon, and T. Petrosky, *Phys. Rev. Lett.* **99**, 210404 (2007); S. Garmon, H. Nakamura, N. Hatano, and T. Petrosky, *Phys. Rev. B* **80**, 115318 (2009).
- [43] E. N. Bulgakov and A. F. Sadreev, *Phys. Rev. B* **78**, 075105 (2008).
- [44] I. Rotter, *J. Phys. A: Math. Theor.* **42**, 153001 (2009).
- [45] N. Moiseyev, *Phys. Rev. Lett.* **102**, 167404 (2009).
- [46] H. Lee and L. E. Reichl, *Phys. Rev. B* **79**, 193305 (2009).
- [47] J. Ping, X.-Q. Li, and S. Gurvitz, *Phys. Rev. A* **83**, 042112 (2011).
- [48] J. M. Zhang, D. Braak, and M. Kollar, *Phys. Rev. Lett.* **109**, 116405 (2012).
- [49] F. Monticone and A. Alù, *Phys. Rev. Lett.* **112**, 213903 (2014).
- [50] Y. Boretz, G. Ordonez, S. Tanaka, and T. Petrosky, *Phys. Rev. A* **90**, 023853 (2014).
- [51] A. González-Tudela and J. I. Cirac, *Phys. Rev. Lett.* **119**, 143602 (2017).
- [52] H. M. Nussenzweig, *Nucl. Phys.* **11**, 499 (1959).
- [53] H. Høegre, *Phys. Lett. A* **201**, 111 (1995).
- [54] N. Moiseyev, *Non-Hermitian Quantum Mechanics* (Cambridge University Press, Cambridge, 2011).
- [55] N. Hatano and G. Ordonez, *J. Math. Phys.* **55**, 122106 (2014).
- [56] C. B. Chiu, B. Misra, and E. C. G. Sudarshan, *Phys. Rev. D* **16**, 520 (1977).
- [57] G. García-Calderón, J. L. Mateos, and M. Moshinsky, *Phys. Rev. Lett.* **74**, 337 (1995).
- [58] R. M. Cavalcanti, *Phys. Rev. Lett.* **80**, 4353 (1998).
- [59] J. G. Muga, V. Delgado, and R. F. Snider, *Phys. Rev. B* **52**, 16381 (1995).
- [60] E. Sánchez-Burillo, D. Zueco, L. Martín-Moreno, and J. J. García-Ripoll, *Phys. Rev. A* **96**, 023831 (2017).
- [61] G. García-Calderón, I. Maldonado, and J. Villavicencio, *Phys. Rev. A* **76**, 012103 (2007).
- [62] C. W. Hsu, B. Zhen, J. Lee, S.-L. Chua, S. G. Johnson, J. D. Joannopoulos, and M. Soljačić, *Nature* **499**, 188 (2013).
- [63] B. Zhen, C. W. Hsu, L. Lu, A. D. Stone, and M. Soljačić, *Phys. Rev. Lett.* **113**, 257401 (2014).
- [64] E. N. Bulgakov and D. N. Maksimov, *Phys. Rev. Lett.* **118**, 267401 (2017).